



**CHALMERS**  
UNIVERSITY OF TECHNOLOGY

## **Edible Film Based on *Lallemantia peltata* L. Seed Gum: Development and Characterization**

Downloaded from: <https://research.chalmers.se>, 2024-05-07 20:32 UTC

Citation for the original published paper (version of record):

Abdolshahi, A., Majd, M., Abdollahi, M. et al (2022). Edible Film Based on *Lallemantia peltata* L. Seed Gum: Development and Characterization. *Journal of Chemical Health Risks*, 12(1): 47-61.  
<http://dx.doi.org/10.22034/jchr.2020.1896596.1118>

N.B. When citing this work, cite the original published paper.



## ORIGINAL ARTICLE

## Edible Film Based on *Lallemantia peltata* L. Seed Gum: Development and Characterization

Anna Abdolshahi<sup>1</sup>, Mojtaba Heydari Majd<sup>2</sup>, Mehdi Abdollahi<sup>3</sup>, Saeideh Fatemizadeh<sup>4</sup>, Leila Monjazez Marvdashti<sup>\*1</sup>

<sup>1</sup>Food Safety Research Center (salt), Semnan University of Medical Sciences, Semnan, Iran

<sup>2</sup>Zabol University of Medical Sciences, Zabol, Iran

<sup>3</sup>Department of Biology and Biological Engineering – Food and Nutrition Science, Chalmers University of Technology, SE 412 96 Gothenburg, Sweden

<sup>4</sup>Department of Food Science and Technology, Ferdowsi University of Mashhad (FUM), Mashhad, Iran

(Received: 15 March 2020

Accepted: 16 May 2020)

## KEYWORDS

Edible films;  
*Lallemantia Peltata*  
(L.);  
Seed gum;  
Thermomechanical  
properties;  
Plasticizer

**ABSTRACT:** A novel edible film was developed using *Lallemantia peltata* (L.) seed gum (LSG), and its water sensitivity, physico-mechanical, barriers, microstructural and thermal properties as a function of glycerol concentration (20, 30, 40, 50 and 60% w/w) were studied. Different models were also used to investigate the water sorption of the LSG films. Unplasticized LSG films were brittle and difficult to handle which were effectively modified by glycerol addition. Water sensitivity, oxygen permeability, and elongation of LSG films were increased with increasing glycerol concentration. Also, increasing of glycerol concentration resulted in reduction of tensile strength, glass transition temperature (T<sub>g</sub>) and melting temperature (T<sub>m</sub>) of the films. Electron scanning micrographs revealed a smooth surface and compact cross-section microstructure in LSG films. The films showed sigmoid shape type II water sorption isotherms, representing typical features of most of biopolymers. Accordingly, the results suggest that LSG films containing desired glycerol concentration could potentially be used as edible films in food packaging.

## INTRODUCTION

The current global application of petroleum-based plastics has to be restricted due to the environmental concerns related to the non-biodegradable nature of plastic letting them persist for thousands of years after disposal. Moreover, they can break down into harmful microfragments which can easily leach into the surrounding environments and be a threat for living organisms [1, 2]. As a promising alternative, biodegradable materials have gained great interest in packaging industries due to their immense advantages compared to the non-biodegradable

plastic films. Edible films offer a way to reduce disposal of plastic packaging as well as extension in the shelf life of foods, and may minimize microbial growth in the product [3-6]. This type of films can be produced using biopolymers included polysaccharides, proteins, and fats; however, carbohydrates are more attractive due to their abundant resources.

In several studies, edible films have been developed using a wide range of polysaccharides, such as chitosan, carrageenan, agar, starch, cellulose, alginate derivatives [7].

\*Corresponding author: leilamonjazez@yahoo.com (L. Monjazez)

Most recently film forming capacity of novel resources such as psyllium seed mucilage [8], tara gum [9], basil seed gum [10], cashew gum [11], and *Lepidiumperfoliatum* seed gum [12] have been also studied.

The genus *Lallemantia*, which belongs to the Lamiaceae family, is one of the medicinal plants that is distributed in various regions of Asia and Europe [13]. *Lallemantia peltata* (L.) Fisch. & C.A.Meyis one of the five species of Iranian flora *Lallemantia* which is distributed in various areas of Iran (North, East North, East South, and Alborz Mountains). *Lallemantia peltata* (L.) seed is used as a traditional medicine in the treatment of joint inflammation, rheumatism, joint pain, abscesses inflammations, and osteoarthritis [14]. Gum extracted from *Lallemantia peltata* (L.) seeds constitutes are carbohydrates (61.74%), crude fiber (29.66%), proteins (0.87%), and ash (8.33%) [15]. The molecular weight and intrinsic viscosity of the gum was  $3.65 \times 10^6 \text{ g mole}^{-1}$  and  $7236.18 \text{ ml g}^{-1}$ , respectively [16]. Furthermore, the potential of LSG as a stabilizing agent has been reported [17]. Considering the various interesting properties, LSG seems to be a promising material for the making of films but to the best of our knowledge, it is not studied yet.

Since polysaccharide films are brittle, addition of polyols is essential to produce efficient and flexible films. Glycerol is such a main preferred polyols in film formation as the glycerol molecules efficiently improve the workability and flexibility properties via diminishing the intermolecular strength in the polymer chains. The extensibility of the films increases after adding glycerol, whereas the barrier properties of the film against water vapour and gas decrease [18]. Thus, optimum concentration of glycerol in a film matrix has effect on the formation of flexible films with proper barrier properties and water sensitivity of the biodegradable films. However, no information has been published on films made with *Lallemantia peltata* (L.) gum and there is no knowledge about the physicochemical and microstructural properties of LSG films. Bearing these, this study was focused on developing and characterizing a novel biodegradable film based on LSG. Also, the effect of various levels (20, 30, 40, 50, 60% (w/w)) of glycerol, as plasticizers, on physical, molecular structure and surface

hydrophobicity, as well as thermal, barrier, mechanical and optical properties of the LSG films was investigated.

## MATERIALS AND METHODS

### Extraction of LSG

LSG was extracted using a sequential process described. [19]. In brief, the cleaned *Lallemantia peltata* (L.) seeds were soaked in distilled water ( $50 \pm 2.0^\circ\text{C}$ ) with a water to seed ratio of 20:1 and mechanically stirred using a magnetic stirrer. The pH of the solution was adjusted to 7 by HCl and/or NaOH ( $0.1 \text{ mol L}^{-1}$ ). After 60 min, the seeds were discarded from the seed–water slurry using an extractor. Thereafter, the slurry was dried at  $50^\circ\text{C}$  for 48 h, and after milling it was sieved using a 100-mesh sifter.

### Film formation

LSG powder (1.5 g) was dissolved in 100 ml of distilled water via mild stirring (300 rpm for 20 min). Temperature was set at  $40^\circ\text{C}$ . Moreover, glycerol (as plasticizer) was added at different concentrations (20, 30, 40, 50, and 60% (w/w)) into the LSG solution. Then, the solutions were stirred at 400 rpm for 20 min. To remove the air bubbles was centrifuged at 10,000 g for 10 min. The prepared solutions were finally cast onto the glass plates (diameter 14 cm) and dried at  $40^\circ\text{C}$  for 15 h. The films were preconditioned in a desiccator containing saturated magnesium nitrate solution creating 52.89% relative humidity at  $25^\circ\text{C}$  until use.

### Physical properties of LSG films

#### Thickness and density assay

A digital micrometre (QLR digital-IP54, China) was used to measure the thickness in five points of film samples randomly and reported as mean values.

To determine the density of film the samples ( $4 \times 4 \text{ cm}$  dimensions) were conditioned in a chamber containing  $\text{P}_2\text{O}_5$  (0% RH) for 5 days. The film density was calculated by the following equation.

$$\rho = \frac{m}{A \times d} \quad (1)$$

where A is film area (16 cm<sup>2</sup>), d is film thickness (cm), and m is film dry mass (g). Film density was expressed as the average of five determinations.

#### Moisture content measurement

The preconditioned films (about 20 mg) were kept in an oven at 105 °C until constant weight. The moisture content (%) was calculated as follows:

$$MC = \frac{m_i - m_d}{m_i} \times 100 \quad (2)$$

where,  $m_i$  and  $m_d$  represent the initial and dried sample weights, respectively. The test was replicated three times.

#### Water solubility measurement

The oven dried film samples were weighed and placed in 50 ml of distilled water under constant agitation at 25 °C. After 6 h, the remaining pieces of the samples were dried at 107 °C to attain the constant weight. The Equation (3) was used to calculate the water solubility (%) of the samples:

$$WS\% = \frac{dw_i - dw_f}{dw_i} \quad (3)$$

where  $dw_i$  and  $dw_f$  are the initial and final dry weights, respectively. Three replicates were analyzed per film formulation.

#### Moisture sorption kinetics and isotherm measurement

A standard gravimetric methodology was used to determine the adsorption kinetics of the samples [20]. Film sheets of 20 × 20 m were initially dried in a vacuum oven at 70°C and 76mmHg for 48 h, and then conditioned at 0% RH (H<sub>2</sub>SO<sub>4</sub>) at 25°C for 72h. After weighing, the dried samples (in triplicate) were conditioned in desiccators with different saturated salt solutions at 25°C. The salt solutions were including LiCl, MgCl<sub>2</sub>, Mg (NO<sub>3</sub>)<sub>2</sub>, NaCl, and KNO<sub>3</sub> that revealed different relative humidities of 11.3, 32.4, 51.4, 75.7, and 92.5%, respectively. The samples were weighed at 24 h intervals until the equilibrium state was reached. The equilibrium moisture were expressed on a dry weight basis (g water/g dry sample).

#### Moisture sorption isotherm modeling

The experimental data of the adsorption isotherms of LSG samples were fitted with the Brunauer–Emmett–Teller (BET) model (Eq. (4)), Guggenheim–Anderson–Boer (GAB) model (Eq. (5)) [21], and Oswin (Eq. (6)) model [22] equations:

$$M_e = \frac{M_0 C a_w}{1 - a_w [1 + (C - 1) a_w]} \quad (4)$$

$$M_e = \frac{M_0 C K a_w}{1 - a_w [1 + (C - 1) k a_w]} \quad (5)$$

$$M_e = k [a_w / (1 - a_w)]^c \quad (6)$$

Where  $M_e$  is the equilibrium moisture content,  $M_0$  is the monolayer moisture value,  $a_w$  is the water activity, and C and k are the equation parameters.

#### Color analysis

The color parameters were determined using a Hunter-Lab (colorFlex EZ, 45°/0°, USA). A white standard plate ( $L^* = 93.49$ ,  $a^* = 0.25$ ,  $b^* = 0.09$ ) was used to calculate the total color difference ( $\Delta E$ ) using the following equation [23]:

$$\Delta E = \sqrt{(L^* - L)^2 + (a^* - a)^2 + (b^* - b)^2} \quad (7)$$

In this equation,  $L^*$ ,  $a^*$ , and  $b^*$  are the color parameters of the film at the background of white standard plate, L (lightness), a (red-green), and b (yellow-blue) are the color parameter of the samples.

#### Opacity measurement

Regarding spectrophotometric method the opacity was measured in film samples [24]. At wavelength of 600 nm the light barrier characteristic of the preconditioned samples were measured considering average of three absorbance readings of each film. Opacity was quantified using equation (8):

$$Opacity = \frac{Abs600}{X} \quad (8)$$

where  $Abs_{600}$  is the value of absorbance at 600 nm and X is the film thickness (mm).

### **Contact angle evaluation**

The sessile drop method was used to estimate surface hydrophilicity. After placing 20  $\mu$ l of distilled water on the film surface, an image was instantly captured by a digital camera. The image was analyzed using Image J Software and contact angles were determined.

### **Water vapor permeability evaluation (WVP)**

According to ASTM E96 standard method the WVP of the film samples was measured [25] regarding air gap inside test cups, described by Shojaee-Aliabadi, et al. [24]. In brief, the film samples were placed and sealed on the opening surface of the circular test cups (10 mm) that were filled with anhydrous calcium chloride (0% RH) then kept in a desiccator containing a saturated solution of sodium chloride (RH 75%). Herein, 75% RH gradient was observed across the films. Weight gain of the cells was monitored over a 48-h period with 2 h intervals to the nearest 0.0001 g as a function of time. WVP of the films was measured by equation (9):

$$WVP = \frac{X \times \Delta m}{A \times \Delta t \times \Delta p} \quad (9)$$

where X is the film thickness (mm),  $\Delta m/\Delta t$  is the weight of the moisture gain per unit of time ( $g\ s^{-1}$ ), A is the area of the film surface ( $m^2$ ), and  $\Delta p$  is the gradient water vapor pressure across the film sides (Pa). WVP measurement was done with three replicates.

### **Oxygen permeability assay**

The ASTM D3985-81 [26] standard method was used to determine the oxygen permeability (OP) of LSG films. In brief, 0.144  $m^2$  open area of a mask was sealed by the film sample and exposed to the oxygen flow. Measurements were performed in three or more replicates.

### **Mechanical properties analysis**

The prepared film samples (100 mm  $\times$  10 mm) were preserved in a chamber at relative humidity of 58% for 1 week according to ASTM [27] using a texture analyzer (Texture Pro. CT V1.6 Build26, Brookfield Engineering Labs, Middleboro, MA, USA). The deformation of each film sample during extension ( $10\ mm\ min^{-1}$ ) in determined distance of machine were recorded. In this base mechanical parameters including tensile strength (TS), elongation at break (EB), and elastic modulus (EM) were determined.

### **Scanning electron microscopy (SEM)**

An electron microscope (EM-3200, KYKY, China) was used to evaluate surface and cross-section of the films under definite condition. The LSG films were cryo-fractured in liquid nitrogen and a sputter coater (SC 1620) was used for gold coating of the samples.

Surface and cross-section of the film samples were analyzed using

### **Fourier-transform infrared spectroscopy**

Fourier-transform infrared (FTIR) spectra of the films were studied using an AVATAR 370 FTIR (Thermo Nicolet, USA). The FTIR spectra of films were recorded in the range of 400–4000  $cm^{-1}$  from an average of 15–16 scans at 2  $cm^{-1}$  resolution.

### **Differential scanning calorimetry (DSC)**

Differential scanning calorimetry (TA Instrument, New Castle, DE, USA) was performed to assess the thermal properties of the LSG films. The samples were scanned between  $-100$  and  $300\ ^\circ C$  with a heating rate of  $10\ ^\circ C\ min^{-1}$ . The melting point ( $T_m$ ) and glass transition temperatures ( $T_g$ ) of the samples were reported. All these properties were determined thrice and the mean value was reported.

### Statistical analysis

The resulting data were analyzed with SAS software (Version 9.1, Statistical Analysis System Institute Inc., Cary, NC, USA) and Microsoft Windows Excel 2007. One-way analysis of variance (ANOVA), and Duncan's multiple range test was employed to interpret data ( $p < 0.05$ ). The Image J and MATLAB (R2014a) software were used to determine the contact angle and fitting experimental data with GAB, BET, and Oswin models.

## RESULTS AND DISCUSSION

### Physical properties of LSG film

Preliminary experiments were performed to determine the minimum level of plasticizer for film preparation. The results revealed that unplasticized LSG films were brittle and difficult to handle. The prepared LSG films were slightly white, transparent, flexible, and homogeneous (Figure 1).

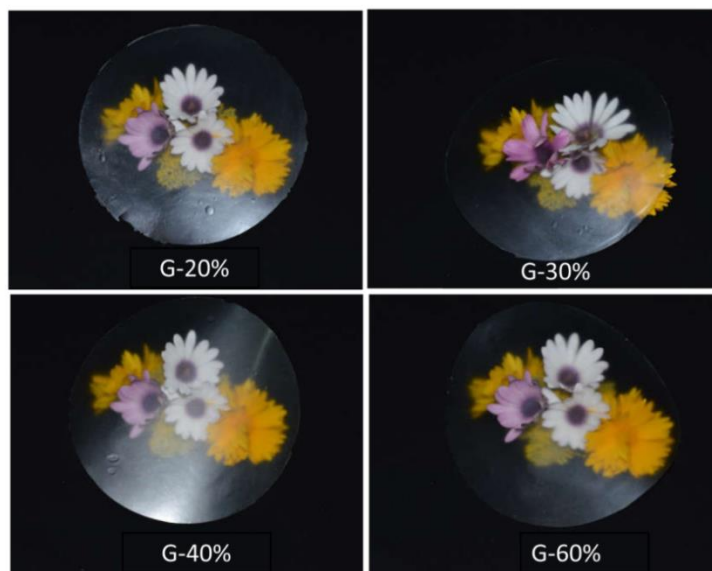


**Figure 1.** The pictorial view of LSG-based films. (Glycerol concentration 20, 30, 40 and 60% w/w)

According to Table 1, the thickness of the LSG film samples increased significantly ( $p < 0.05$ ) in the range of 0.06–0.083 mm as a response to increasing glycerol concentration from 20 to 60% w/w. These results could be attributed to the penetration of the glycerol molecules between polymer chains of the films which can possibly break molecular interactions between the functional groups of LSG chains, leading absorption of more water vapour into the film matrix and increase films thickness [28]. Similar results were observed for sage seed gum-based films [29]. The density of the LSG films decreased

significantly ( $p > 0.05$ ) by increasing glycerol concentration (Table 1). It might be related to the fact that incorporating glycerol into the LSG matrix decreased the intermolecular interactions between the polymer chains, whereas formation of hydrogen bonds between the LSG polymer chains and glycerol molecules were enhanced. This phenomenon might have increased the free volume of the film network and decreased the film density. The results coincide with those previously reported [30] and [12] for films based on cress seed mucilage and *Lepidium perfoliatum* seed gum, respectively.

**Table 1.** Physical properties of LSG films as a function of glycerol concentration

Glycerol concentration (%)	Thickness (mm)	Density (g cm <sup>-3</sup> )	Moisture (%)	Solubility (%)
Without plasticizer	0.060 ± 0.002 <sup>c</sup>	1.38 ± 0.03 <sup>a</sup>	10.92 ± 0.29 <sup>f</sup>	18.01 ± 0.34 <sup>d</sup>
20	0.061 ± 0.001 <sup>c</sup>	1.35 ± 0.02 <sup>a</sup>	13.10 ± 0.2 <sup>e</sup>	18.02 ± 0.56 <sup>d</sup>
30	0.068 ± 0.002 <sup>b</sup>	1.33 ± 0.03 <sup>ab</sup>	17.81 ± 0.31 <sup>d</sup>	20.4 ± 0.53 <sup>c</sup>
40	0.067 ± 0.00 <sup>b</sup>	1.29 ± 0.06 <sup>abc</sup>	23.24 ± 0.28 <sup>c</sup>	22.09 ± 0.59 <sup>b</sup>
50	0.069 ± 0.00 <sup>b</sup>	1.25 ± 0.01 <sup>bc</sup>	25.00 ± 0.25 <sup>b</sup>	21.62 ± 0.40 <sup>b</sup>
60	0.083 ± 0.003 <sup>a</sup>	1.20 ± 0.06 <sup>c</sup>	32.85 ± 0.26 <sup>a</sup>	48.05 ± 0.42 <sup>a</sup>

\*Values are given as mean ± standard deviation. Values within each column with different letters are significantly different ( $p < 0.05$ ).

Moisture content of the LSG-based films was also significantly ( $p < 0.05$ ) affected by glycerol concentration (Table 1). With the increasing glycerol concentration, the moisture content of the LSG films increased significantly because glycerol as a hydrophilic molecule has high affinity toward water molecules. In addition, the number of hydrogen bonds between LSG and glycerol molecules might have increased in the film network by raising the glycerol concentration; hence, the availability of the functional groups to water molecules was enhanced. Similar results were also reported [8] and [29], for films made of psyllium seed (*Plantago ovata*), and sage seed gum, respectively.

The water solubility of the films is an essential property of the edible films that indicates their resistance in high relative humidity environments. The LSG films solubility significantly ( $p < 0.05$ ) increased with increasing glycerol concentration (Table 1). The intramolecular interactions between the biopolymer molecules have possibly decreased and the free volume has increased with the addition of glycerol. This might have caused the increase in solubility of the LSG film. The values of water solubility determined in this study were close to the solubility of edible gum

cordia film[31], but higher than those of films from tara gum[9], and lower than the films of psyllium gum [8], quince seed gum [32], basil seed (*Ocimum basilicum L.*) gum [10], sage seed gum [29] and *Lepidium perfoliatum* seed gum [12].

#### Moisture sorption isotherm

The water sorption isotherm reveals valuable details about the microstructure of films [33]. Figure 2 presents the water sorption isotherms of LSG films prepared with various glycerol concentrations. All curves were in sigmoid shape, indicating type II isotherms that are typical features for most biopolymer materials. The moisture adsorption was rapid at the initial stage of the curves and with increasing time, the value declined until it reached zero (moisture content of the films equilibrated with the RH in each condition). With the increasing glycerol concentration, the adsorbed moisture increased due to the enhancement in the hygroscopic nature of the films and it formed glycerol rich domains in the film matrix. Therefore, the penetration of water molecules into the film network fascinated with the increasing moisture uptake. The results were in line with those reported [34] for corn starch-based edible films.

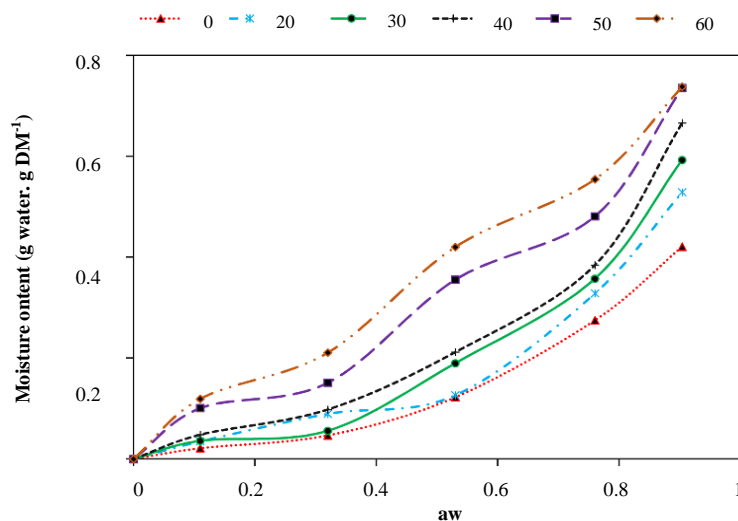


**Figure 2.** Moisture sorption curves of LSG films with different glycerol concentration at various  $a_w$ . (Glycerol concentration from 20 to 60% w/w).

Several models have been used to consider the relationship between  $a_w$  and equilibrium moisture content. One of the most important parameters that affected the food deterioration is the monolayer moisture [35]. BET isotherm equation is the most commonly used model and provides efficient results in 0.05–0.5  $a_w$  for several food species which is based on the absorption of the water monolayer [36]. GAB model is the most versatile sorption model available in the literature and has been applied in many food materials and natural biopolymers. The GAB model is an extended form of the BET model and can adequately describe the moisture sorption isothermal behavior of all foods from 0 to 0.9  $a_w$  [37]. Oswin is another model that is purely empirical [22]. These three models were used to identify the best model for explaining the water sorption of LSG films with different concentrations of glycerol.

The obtained parameters from fitting the experimental data to GAB, BET, and Oswin sorption equations are presented in Table 2. The linearity of the moisture sorption curve of LSG film was excellent because the correlation of determination ( $R^2$ ) for all models was high.

The value of parameter  $M_0$  for GAB and BET models, indicating monolayer water, ranged between 0.7–1.05 and 0.067–0.22 g water/g dry weight, respectively. These estimated values for  $M_0$  are within the reported values for soy protein isolate/carboxymethyl chitosan blend [38] and cassava flour films [39]. The monolayer water increased with the increasing glycerol concentration. This might be due to the increasing active sites for water adsorption. Moreover, the  $M_0$  for the GAB model is higher than the BET model.

With increasing glycerol concentration from 20% to 60% (w/v), the GAB monolayer heat sorption parameter,  $C$ , increased from 1.77 to 2.37 indicating an increase in the magnitude difference of the upper and monolayer. A similar result was reported [40] for cassava flour film. These results might be attributed to the change in the sorption pattern induced by the presence of this polar molecule in the film matrix. Similar to the GAB and BET models, the Oswin model also efficiently describes the moisture isotherms.



**Table 2.** Parameters of GAB, BET and Oswin models obtained for LSG films with different glycerol concentration

Glycerol concentration %	GAB				BET			Oswin		
	M <sub>0</sub>	C	k	R <sup>2</sup>	M <sub>0</sub>	C	R <sup>2</sup>	C	k	R <sup>2</sup>
20	0.074	0.20	1.03	0.98	0.006	0.89	0.92	0.58	0.14	0.98
30	0.083	0.22	1.01	0.99	0.011	1.97	0.96	0.58	0.16	0.99
40	0.084	0.23	1.00	0.99	0.013	2.81	0.98	0.56	0.18	0.99
50	0.093	0.48	0.94	0.98	0.020	3.42	0.93	0.43	0.28	0.97
60	0.096	0.54	0.86	0.99	0.022	5.38	0.97	0.35	0.34	0.95

### Color analysis

Color is an essential parameter for edible films due to their direct influence on the product appearance and consumers' acceptance of packaged food [41]. With increasing glycerol concentration,  $L^*$  and  $b^*$  parameters increased, whereas  $a^*$  and  $\Delta E$  parameters significantly decreased ( $p < 0.05$ ; Table 3) indicating a lightened film appearance. Glycerol addition up to 50% decreased total color difference ( $\Delta E$ ), whereas in higher content, it increased  $\Delta E$ . These results could be attributed to fact that glycerol is a color less component and

dilution of film components as a result of increasing its concentration in the film-forming solution, leading to the increasing of films' lightness [41]. Also, these results may be occurred due to the enhancement of light reflection on the film surface with increasing glycerol concentration. Similar results were also reported [12], indicating that increasing glycerol concentration in film made of cross seed carbohydrate gum, decreased  $a$  value, whereas,  $b$  and  $L$  values increased.

**Table 3.** Color attributes of of-LSG films as a function of glycerol concentration.

Glycerol concentration %	L <sup>*</sup>	a <sup>*</sup>	b <sup>*</sup>	$\Delta E$
20	88.45 ± 0.06 <sup>e</sup>	4.91 ± 0.01 <sup>a</sup>	0.02 ± 0.00 <sup>d</sup>	6.43 ± 0.14 <sup>a</sup>
30	89.24 ± 0.02 <sup>d</sup>	3.74 ± 0.03 <sup>b</sup>	0.03 ± 0.01 <sup>d</sup>	5.08 ± 0.07 <sup>b</sup>
40	91.27 ± 0.03 <sup>c</sup>	3.25 ± 0.04 <sup>c</sup>	0.09 ± 0.01 <sup>c</sup>	3.26 ± 0.10 <sup>c</sup>
50	94.27 ± 0.03 <sup>b</sup>	0.78 ± 0.03 <sup>d</sup>	0.15 ± 0.02 <sup>b</sup>	0.85 ± 0.39 <sup>e</sup>
60	94.35 ± 0.04 <sup>a</sup>	0.03 ± 0.01 <sup>e</sup>	0.19 ± 0.00 <sup>a</sup>	1.22 ± 0.09 <sup>d</sup>

\*Values are given as mean ± standard deviation. Values within each column with different letters are significantly different ( $p < 0.05$ ).

### Film opacity

Transparency of packaging is an important property, as the increased tendency to view the product clearly within the packaging. As presented in Table 4, with increasing glycerol concentration, the opacity of the LSG films significantly decreased ( $p < 0.05$ ). The obtained opacity values for the LSG film were comparatively lower than those reported for the brea gum film [42]. In general, film

thickness and structure determine the opacity of the film. Therefore, increasing film thickness, by addition of glycerol, may have decreased the opacity of the film. Similar behavior was reported [12] for films of *Lepidium perfoliatum* seed gum. This result suggests that glycerol was blended homogeneously with the LSG and was fully embedded in its network (Figure 1).

**Table 4.** Oxygen permeability (OP), contact angle (CA), water vapor permeability (WVP) and opacity of LSG films as a function of glycerol concentration

Glycerol concentration %	OP (cm <sup>3</sup> μm/(m <sup>2</sup> d kPa))	CA	WVP (g/m s Pa)	Opacity
Without plasticizer	-	80.08± 0.3 <sup>a</sup>	-	10.12 ± 0.5 <sup>a</sup>
20	11.25± 0.04 <sup>e</sup>	78.1± 0.3 <sup>b</sup>	1.5± 0.02 <sup>e</sup>	7.31± 0.22 <sup>b</sup>
30	11.32± 0.01 <sup>d</sup>	76.54± 0.3 <sup>c</sup>	1.63± 0.03 <sup>d</sup>	5.42± 0.47 <sup>c</sup>
40	11.53± 0.03 <sup>e</sup>	75.34± 0.3 <sup>d</sup>	1.78± 0.04 <sup>c</sup>	6.18± 0.05 <sup>e</sup>
50	12.06± 0.02 <sup>b</sup>	74.6± 0.3 <sup>e</sup>	1.97± 0.04 <sup>b</sup>	6.47± 0.08 <sup>e</sup>
60	12.41± 0.02 <sup>a</sup>	48.2± 0.3 <sup>f</sup>	2.29± 0.02 <sup>a</sup>	6.46± 0.86 <sup>bc</sup>

\*Values are given as mean ± standard deviation. Values within each column with different letters are significantly different ( $p < 0.05$ ).

### Contact angle

The contact angle (CA) of water is also an important issue in materials intended for packaging materials, indicating surface hydrophilic/hydrophobic properties of the packaging. In general, lower angles represent high hydrophilic surface. It is known that the contact angle may be changed from 0° to 180° (0° refers to the whole spreading of the liquid and 180° indicates the limit of entirely no wetting) [43]. Contact angle of the LSG film samples plasticized by different concentrations of glycerol are presented in Table 4. A significant difference was observed among the distilled water contact angles for the films with different concentrations of glycerol ( $p < 0.05$ ). Increasing glycerol concentration as plasticizer led to a significant decrease in the contact angle from 80.08° to 48.2°. W contact angles of the LSG-based films ranged between 30° and 90°. Therefore, these films were partially wetting and revealed the behavior similar to polysaccharide-based edible films [43]. Similar results have been stated about influence of the plasticizer concentration on contact angle of *Alyssum homolocarpum* seed gum-polyvinyl alcohol biodegradable composite film [44].

### Water vapour permeability

Avoiding mass transfer is a crucial feature of a biodegradable polymer when used as a packaging material. Thus, a good barrier against aroma, water vapor, and gases is generally preferred. Therefore, WVP is the most important barrier property that usually evaluates the biodegradable films due to its close relation with the deteriorative reactions. As presented in Table 4, increasing

glycerol concentration significantly enhanced the WVP of the LSG edible film ( $p < 0.05$ ). WVP of the LSG-based film without glycerol was not determined due to its brittle structure. In general, increasing the hydrophilicity of the polymer matrix increases the WVP of a hydrocolloid film [45]; hence, since addition of plasticizers elevate hydrophilic nature of a matrix eventually enhance WVP. Similar results have been reported for films made of cassava starch [46], gum [9], flaxseed gum-based edible [47] and gum cordia [31] as a function of plasticizer addition. The obtained WVP for LSG films in this work was close to WVP of basil seed (*Ocimum basilicum L.*) gum films elaborated [10], who determined the WVP in the range of  $1.66$  to  $2.24 \times 10^{-10}$  g H<sub>2</sub>O m<sup>-2</sup> s<sup>-1</sup> MPa<sup>-1</sup>.

### Oxygen permeability (OP)

The effect of the plasticizer concentration on the OP of the LSG edible films are shown in Table 4. Based on glycerol concentration increase, the OP of the LSG films increased from 11.25 to 12.41 cm<sup>3</sup> mm/m<sup>2</sup>d<sup>1</sup> kPa<sup>1</sup>. Several factors have effect on OP of a film such as the physical and chemical properties also the molecular weight of the plasticizer, the interaction between plasticizer and the oxygen and the structure of film in a complex manner [31]. In comparison to LSG (MW =  $3.65 \times 10^6$  g mol<sup>-1</sup>), glycerol is a smaller molecule that easily penetrates the film network and decreases attractive forces between the LSG macromolecules. Thus, it creates a film network with higher free volume space in its structure [16] which facilitates the penetration and transition of gas molecules

across the film [48]. Similar results were also obtained for quince seed mucilage film [32]. The average oxygen permeability value ( $11.71 \text{ cm}^3 \mu\text{m} / \text{m}^2 \text{ d kPa}$ ) of the LSG-based film was higher than those reported [49] and [50] for films based on starch and polyvinylidene chloride, respectively, whereas higher OP was recorded for chitosan film [51].

### Mechanical properties

The mechanical properties of the LSG films including tensile strength (TS) and elongation at break (EB) were studied and the results are presented in Table 5. The TS of the LSG film decreased prominently from 78.31 to 18.98

MPa, on increasing the glycerol concentration from 20 to 60% w/w ( $p < 0.05$ ; Table 5). The elasticity of the LSG film was evaluated using elongation at break, in which the results revealed significant increase in this parameter with the increasing glycerol concentration [52]. Glycerol decreased the rigidity and increased the flexibility of the polymer network due to reduction in the intramolecular interactions between the polymer molecules [53]. In addition, increasing moisture content of the film may have caused a plasticizing effect on the film structure because the water molecules can act as plasticizing agent and enhance the mobility of the polymer chains and EB%.

**Table 5.** Glass transition temperature ( $T_g$ ), melting temperature ( $T_m$ ) and mechanical properties of LSG films as a function of glycerol concentration

Glycerol concentration % (w/w)	$T_g$ ( $^{\circ}\text{C}$ )	$T_m$ ( $^{\circ}\text{C}$ )	TS (MPa)	EB (%)
20	$16.38 \pm 1.04^d$	$105.69 \pm 0.50^a$	$78.31 \pm 3.34^a$	$9.24 \pm 1.02^d$
30	$-29.42 \pm 1.10^e$	$103.6 \pm 2.05^{bc}$	$54.91 \pm 2.11^b$	$17.13 \pm 2.50^e$
40	$-48.94 \pm 0.92^c$	$101.24 \pm 1.20^{ab}$	$45.45 \pm 4.65^c$	$20.58 \pm 2.19^{ab}$
50	$-63.86 \pm 1.82^a$	$100.92 \pm 2.90^d$	$31.23 \pm 1.79^d$	$24.08 \pm 1.73^b$
60	$-69.77 \pm 0.40^b$	$100.11 \pm 2.01^c$	$18.98 \pm 2.12^e$	$50.04 \pm 3.31^a$

\*Values are given as mean  $\pm$  standard deviation. Values within each column with different letters are significantly different ( $p < 0.05$ ).

Based on the mechanical properties results, it could be concluded that an increase in the glycerol concentration of the LSG films, improved the film extensibility and reduced its resistance. Based on the obtained results, LSG film with 40% glycerol revealed the best mechanical properties.

### Film microstructure

SEM can reveal film homogeneity, surface microstructure, pores, cracks, surface smoothness, and thickness of a film. Moreover, it can help to find of relationships between films structure with water vapor transmission, mechanical, and optical properties. Figure 3 presents the cross-sections and surface SEM micrographs of the LSG films with different

concentrations of glycerol. SEM micrograph of the LSG films, incorporated with glycerol, revealed smooth and uniform surfaces without any crack or pore. Cross-sections of the LSG films indicated that the addition of the plasticizer, improved homogeneity of the film structure without noticeable cracks and breaks. Surface micrographs also revealed that the use of glycerol improved the structure of the LSG films (without pores or cracks and homogeneous) despite its negative effect on barrier properties against water and oxygen molecules. Similar behavior has been reported for films based on quince seed mucilage [32] and yam starch [54] plasticized with glycerol.

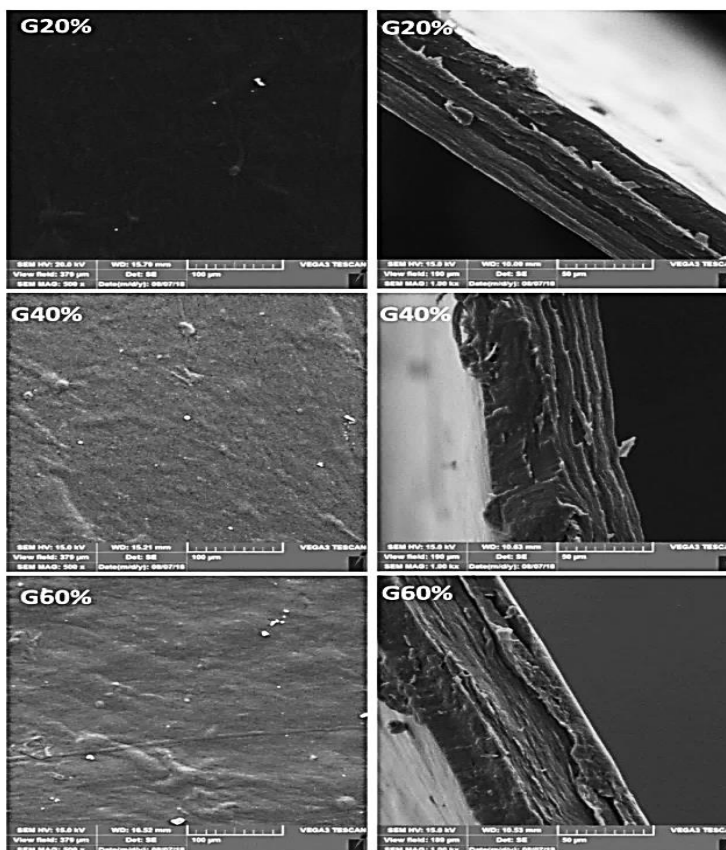


**Figure 3.** Scanning electron micrographs of surface (left) and cross-section (right) of LSG films as a function of glycerol concentration.

#### *Fourier-transform infrared spectroscopy*

FTIR is a useful technique to help micro structural characterization of films since it can help to evaluate the interactions between film components[55]. Figure 4 shows the IR spectrums of LSG films containing 20, 30, 40, 50, and 60% w/w of glycerol. A broad peak located approximately at  $3409.22\text{ cm}^{-1}$  was attributed to the stretching vibration of the OH groups, which was affected by inter- and intermolecular hydrogen bonds. Meanwhile, the CH aliphatic absorption peaks are located around  $2800\text{--}3000\text{ cm}^{-1}$ . The peaks at  $3409\text{ cm}^{-1}$  and  $2895\text{--}2988\text{ cm}^{-1}$  shifted slightly toward the higher wave numbers by increasing glycerol concentration. With increasing glycerol concentration, the intensity of the OH band increased which is due to the increase in the number of free OH groups of glycerol molecules [31] in the LSG film network. Furthermore, this observation may be attributed to the increasing moisture content of the films formulated with more concentrated glycerol. In general, possible types of

hydrogen bonds in a film network may be present between the polymer hydroxyl groups, between the polymer hydroxyl group and glycerol hydroxyl group, and between hydroxyl groups within the glycerol. Energies of these bonds are different. Presumably, at lower concentration of glycerol, all the hydroxyl groups of the polymer interacted with the hydroxyl group of the glycerol molecules; hence, the polymer-polymer interaction is replaced to polymer-plasticizer interactions. This phenomenon is called the solvation effect of the plasticizer [31]. These results indicate that the increasing glycerol content altered the nature of the hydrogen bonding in the films. Increasing glycerol concentration lead to a shift of the peak at  $1620.86\text{ cm}^{-1}$  (presented in LSG films without glycerol), to lower wavenumbers. Furthermore, the characteristic peak around  $1456\text{ cm}^{-1}$  resulted essentially from the presence of glycerol [56]. This glycerol band shifted to the lower wavenumbers in the LSG film matrix, which indicate

hydrogen bands between the glycerol molecules and LSG polymer chains.

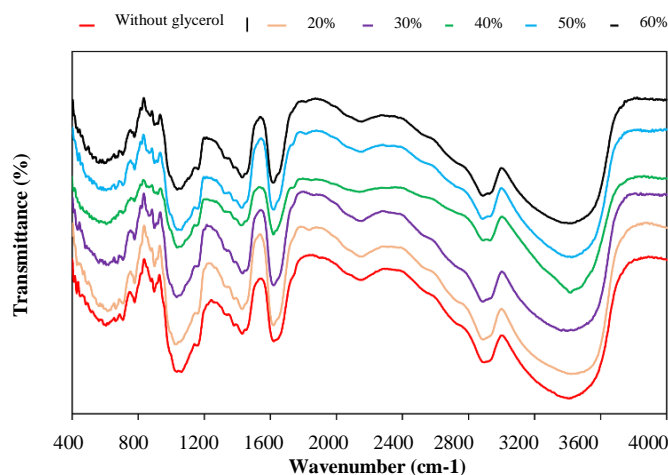


Figure 4. FTIR spectra of LSG films as a function of glycerol concentration.

Results revealed that the interaction between the film ingredients changed with increasing glycerol concentration and produced an open network with higher water molecules and lower hydrogen bond between the LSG polymer chains.

#### Thermal properties

As presented in Table 5, the  $T_g$  and  $T_m$  values of the LSG films significantly decreased with increasing glycerol concentration, ( $p < 0.05$ ). The LSG film with 20% glycerol had a  $T_g$  higher than zero indicating that the structure of film was brittle at the room temperature. As mentioned before, glycerol is a polar molecule with low molecular weight that can penetrate among LSG polymers and decrease their intermolecular interactions. Therefore, the free volumes of film network and polymer chains mobilities were increased. Similar results were observed for films based on *Alyssum homolocarpum* seeds gum-PVA [44], with high  $T_g$  values at unplasticized films. These results supported the observation about density and mechanical properties revealing that the LSG films were more homogeneous when the glycerol concentration increased. Moreover, with increasing glycerol concentration, due to the hydrophilic nature of glycerol, the moisture content of the LSG films increased (Table 1). Water molecules have a plasticizing effect; hence, they can decrease the  $T_m$  and  $T_g$  values [31].

#### CONCLUSIONS

This is the first report on the feasibility of edible films and coatings development from LSG. However, the LSG film without plasticizer was brittle and difficult to handle. LSG film with 20% of glycerol had the lowest water solubility, WVP, OP, moisture content, moisture adsorption, water solubility, and highest opacity. The elasticity of the film increased by the addition of glycerol and it consequently improved the mechanical properties of the film and LSG film with 40% glycerol revealed the best mechanical properties. The BET, GAB, and Oswin models were found to be effective models for this film throughout the range of water activity. The findings of the present study demonstrated that LSG had a good potential, as an alternative carbohydrate, to develop new edible films for packaging of food products containing low moisture or dried. Further investigations are needed to modify LSG films properties by addition of essential oils, nanoparticles and etc.

#### ACKNOWLEDGEMENTS

The authors appreciate of Cooperation Semnan University of Medical Sciences and Food Safety Research Center (salt).

## ETHICAL CONSIDRATION

The study project had approved by the research ethics committee of Semnan University of Medical Sciences (approval ID: IR.SEMUMS.REC.1399.127). The authors appreciate of Cooperation Semnan University of Medical Sciences and Food Safety Research Center (salt).

### Conflicts of interest

The authors declare no conflicts of interest.

## REFERENCES

- Heydari-Majd M., Ghanbarzadeh B., Shahidi-Noghabi M., Najafi M.A., Adun P., Ostadrahimid A.J.P.T., 2019. Kinetic release study of zinc from polylactic acid based nanocomposite into food simulants. *Polymer Testing*. 1;76, 254-60.
- Marvdashti L.M., Koochehi A., Yavarmanesh M.J.C.P., 2017. Alyssum homolocarpum seed gum-polyvinyl alcohol biodegradable composite film: Physicochemical, mechanical, thermal and barrier properties. *Carbohydrate Polymers*. 155, 280-293.
- Heydari-Majd M., Ghanbarzadeh B., Shahidi-Noghabi M., Najafi M.A., Hosseini M.J.F.P., Life S., 2019. A new active nanocomposite film based on PLA/ZnO nanoparticle/essential oils for the preservation of refrigerated *Otolithes ruber* filets. *Food Packaging and Shelf Life*. 19, 94-103.
- Marvdashti L.M., Koochehi A., Yavarmanesh M.J.F.B., 2019. Characterization, Release Profile and Antimicrobial Properties of Bioactive Polyvinyl Alcohol-Alyssum homolocarpum Seed Gum-Nisin Composite Film. *Food Biophysics*. 15;14(2), 120-31
- Abdolshahi A., Marvdashti L.M., Salehi B., Sharifi - Rad M., Ghobakhloo S., Iriti M., Sharifi - Rad J., 2019. Antifungal activities of coating incorporated with *Saccharomyces cerevisiae* cell wall mannoprotein on *Aspergillus flavus* growth and aflatoxin production in pistachio (*Pistacia vera* L.). *Journal of Food Safety*. 39(2), e12608.
- Abdolshahi A., Tabatabaei Yazdi F., Shabani A., Mortazavi S., 2019. Active gelatin-mannan film: physicochemical, antifungal and aflatoxin binding properties. *International Food Research Journal*. 26(6), 1803-1812.
- Monjazebe Marvdashti L., Abdulmajid Ayatollahi S., Salehi B., Sharifi- Rad J., Abdolshahi A., Sharifi- Rad R., Maggi F., 2020. Optimization of edible Alyssum homolocarpum seed gum- chitosan coating formulation to improve the postharvest storage potential and quality of apricot (*Prunus armeniaca* L.). *Journal of Food Safety*:e12805.
- Ahmadi R., Kalbasi-Ashtari A., Oromiehie A., Yarmand M.S., Jahandideh F., 2012. Development and characterization of a novel biodegradable edible film obtained from psyllium seed (*Plantago ovata* Forsk). *Journal of Food Engineering*. 109(4), 745-751.
- Antoniou J., Liu F., Majeed H., Qazi H.J., Zhong F., 2014. Physicochemical and thermomechanical characterization of tara gum edible films: effect of polyols as plasticizers. *Carbohydrate Polymers*. 111, 359-365.
- Khazaei N., Esmaili M., Djomeh Z.E., Ghasemlou M., Jouki M., 2014. Characterization of new biodegradable edible film made from basil seed (*Ocimum basilicum* L.) gum. *Carbohydrate Polymers*. 102, 199-206.
- Moreira B.R., Batista K.A., Castro E.G., Lima E.M., Fernandes K.F., 2015. A bioactive film based on cashew gum polysaccharide for wound dressing applications. *Carbohydrate polymers*. 122, 69-76.
- Seyedi S., Koochehi A., Mohebbi M., Zahedi Y., 2014. *Lepidium perfoliatum* seed gum: A new source of carbohydrate to make a biodegradable film. *Carbohydrate Polymers*. 101, 349-358.
- Ghannadi A., Zolfaghari B., 2003. Compositional analysis of the essential oil of *Lallemantia royleana* (Benth. in Wall.) Benth. from Iran. *Flavour and Fragrance Journal*. 18(3), 237-239.
- Moghaddam T.M., Razavi S., Emadzadeh B., 2011. Rheological interactions between *Lallemantia royleana* seed extract and selected food hydrocolloids. *Journal of the Science of Food and Agriculture*. 91(6), 1083-1088.

15. Mohammad Amini A., 2007. Extraction optimization of Balangu seed gum and effect of Balangu seed gum on the rheological and sensory properties of Iranian flat bread (Doctoral dissertation, MSc thesis, Ferdowsi University of Mashhad, Iran), 14-28.
16. Amini A.M., Razavi S.M., 2012. Dilute solution properties of Balangu (*Lallemantia royleana*) seed gum: Effect of temperature, salt, and sugar. International Journal of Biological Macromolecules. 51(3), 235-243.
17. Najafi M.N., Hosaini V., Mohammadi-Sani A., Koocheki A., 2016. Physical stability, flow properties and droplets characteristics of Balangu (*Lallemantia royleana*) seed gum/whey protein stabilized submicron emulsions. Food Hydrocolloids. 59, 2-8.
18. Baldwin E. A., Hagenmaier R., Bai J., 2011. Edible coatings and films to improve food quality. CRC Press. Book. Aug 24. 17-36
19. Salehi F., Kashaninejad M., Behshad V., 2014. Effect of sugars and salts on rheological properties of Balangu seed(*Lallemantia royleana*) gum. International Journal of Biological Macromolecules. 67 16-21.
20. Farahnaky A., Ansari S., Majzoobi M., 2009. Effect of glycerol on the moisture sorption isotherms of figs. Journal of Food Engineering. 93(4), 468-473.
21. Berg C., Bruin S., 1981. Water activity and its estimation in food systems: theoretical aspects. In Rockland LB, Stewart GF, editors, Water activity: Influences on food quality. New York: Academic Press. 2-61.
22. Oswin C., 1946. The kinetics of package life. III. The isotherm. Journal of Chemical Technology and Biotechnology. 65 (12), 419-421.
23. Bonilla J., Fortunati E., Atarés L., Chiralt A., Kenny J.M., 2014. Physical, structural and antimicrobial properties of poly vinyl alcohol–chitosan biodegradable films. Food Hydrocolloids. 35, 463-470.
24. Shojaee-Aliabadi S., Hosseini H., Mohammadifar M.A., Mohammadi A., Ghasemlou M., Ojagh S.M., Hosseini S.M., Khaksar R., 2013. Characterization of antioxidant-antimicrobial  $\kappa$ -carrageenan films containing Satureja hortensis essential oil. International Journal of Biological Macromolecules. 52, 116-124.
25. ASTM E., 1995. Standard test methods for water vapor transmission of materials. Foundation drainage rate: Hydraulic Gradient, 1, 18.
26. ASTM D3985-81, 2002. D3985-81. Oxygen gas transmission rate through plastic film and sheeting using a coulometric sensor.
27. ASTM D., 2002. 882-02. Standard test method for tensile properties of thin plastic sheeting.
28. Sadeghi-Varkani A., Emam-Djomeh Z., Askari G., 2018. Physicochemical and microstructural properties of a novel edible film synthesized from Balangu seed mucilage. International Journal of Biological Macromolecules. 108, 1110-1119.
29. Razavi S.M.A., Amini A.M., Zahedi Y., 2015. Characterisation of a new biodegradable edible film based on sage seed gum: Influence of plasticiser type and concentration. Food Hydrocolloids. 43, 290-298.
30. Jouki M., Khazaei N., Ghasemlou M., HadiNezhad M., 2013. Effect of glycerol concentration on edible film production from cress seed carbohydrate gum. Carbohydrate Polymers. 96 (1), 39-46.
31. Haq M.A., Hasnain A., Azam M., 2014. Characterization of edible gum cordia film: Effects of plasticizers. LWT-Food Science and Technology. 55(1), 163-169.
32. Jouki M., Yazdi F.T., Mortazavi S.A., Koocheki A., 2013. Physical, barrier and antioxidant properties of a novel plasticized edible film from quince seed mucilage. International Journal of Biological Macromolecules. 62, 500-507.
33. Su J.F., Huang Z., Zhao Y.H., Yuan X.Y., Wang X.Y., Li M., 2010. Moisture sorption and water vapor permeability of soy protein isolate/poly (vinyl alcohol)/glycerol blend films. Industrial Crops and Products. 31 (2), 266-276.
34. Ghanbarzadeh B., Almasi H., 2011. Physical properties of edible emulsified films based on carboxymethyl cellulose and oleic acid. International journal of biological Macromolecules. 48(1), 44-49.
35. Zhang Y., Han J., 2008. Sorption isotherm and plasticization effect of moisture and plasticizers in pea starch film. Journal of Food Science. 73(7), E313-24.
36. Brunauer S., Emmett P.H., Teller E., 1938. Adsorption

- of gases in multimolecular layers. *Journal of the American Chemical Society*. 60 (2), 309-319.
37. Cho S.Y., Rhee C., 2002. Sorption characteristics of soy protein films and their relation to mechanical properties. *LWT-Food Science and Technology*. 35(2), 151-157.
38. Rachtanapun P., Suriyatem R., 2012. Moisture sorption isotherms of soy protein isolate/carboxymethyl chitosan blend films. *Journal of Agricultural Science and Technology*. A, 2 (1A), 50.
39. Suppakul P., Chalernsook B., Ratisuthawat B., Prapasitthi S., Munchukangwan N., 2013. Empirical modeling of moisture sorption characteristics and mechanical and barrier properties of cassava flour film and their relation to plasticizing–antiplasticizing effects. *LWT-Food Science and Technology*. 50 (1), 290-297.
40. Suppakul P., 2006. Moisture sorption characteristics of cassava flour film. In *Proceedings of 15th IAPRI World Conference on Packaging*. 1,1-13.
41. Ramos Ó.L., Reinas I., Silva S.I., Fernandes J.C., Cerqueira M.A., Pereira R.N., Vicente A.A., Poças M.F., Pintado M., Malcata F.X., 2013. Effect of whey protein purity and glycerol content upon physical properties of edible films manufactured therefrom. *Food Hydrocolloids*. 30(1), 110-122.
42. Slavutsky A.M., Bertuzzi M.A., Armada M., García M.G., Ochoa N.A., 2014. Preparation and characterization of montmorillonite/brea gum nanocomposites films. *Food Hydrocolloids*. 35, 270-278.
43. Ghanbarzadeh B., Oromiehie A., Musavi M., Falcone P.M., Rad E.R., 2007. Study of mechanical properties, oxygen permeability and AFM topography of zein films plasticized by polyols. *Packaging Technology and Science*. 20(3), 155-163.
44. Monjazeb Marvdashti L., Yavarmanesh M., Koocheki A., 2016. The Effect of Different Concentrations of Glycerol on Properties of Blend Films Based on Polyvinyl Alcohol-AllysumHomolocarpum Seed Gum. *Iranian Food Science and Technology Research Journal*. 12(5), 663-677.
45. Marvdashti L.M., Koocheki A., Yavarmanesh M., 2017. Alyssum homolocarpum seed gum-polyvinyl alcohol biodegradable composite film: Physicochemical, mechanical, thermal and barrier properties. *Carbohydrate Polymers*. 155, 280-293.
46. Müller C.M., Yamashita F., Laurindo J.B., 2008. Evaluation of the effects of glycerol and sorbitol concentration and water activity on the water barrier properties of cassava starch films through a solubility approach. *Carbohydrate Polymers*. 72(1), 82-87.
47. Wang Y., Li D., Wang L.j., Yang L., Özkan N., 2011. Dynamic mechanical properties of flaxseed gum based edible films. *Carbohydrate Polymers*. 86(2), 499-504.
48. Jia D., Fang Y., Yao K., 2009. Water vapor barrier and mechanical properties of konjac glucomannan–chitosan–soy protein isolate edible films. *Food and Bioproducts Processing*. 87(1), 7-10.
49. Gaudin S., Lourdin D., Forssell P., Colonna P., 2000. Antiplasticisation and oxygen permeability of starch–sorbitol films. *Carbohydrate Polymers*. 43(1), 33-37.
50. McHugh T.H., Krochta J.M., 1994. Milk-protein-based edible films and coatings. *Food Technology*. 48(1), 97-103.
51. Di Pierro P., Sorrentino A., Mariniello L., Giosafatto C.V.L., Porta R., 2011. Chitosan/whey protein film as active coating to extend Ricotta cheese shelf-life. *LWT-Food Science and Technology*. 44(10), 2324-2327.
52. Liu H., Adhikari R., Guo Q., Adhikari B., 2013. Preparation and characterization of glycerol plasticized (high-amylose) starch–chitosan films. *Journal of Food Engineering*. 116(2), 588-597.
53. Pongjanyakul T., Puttipipatkachorn S., 2007. Alginate-magnesium aluminum silicate films: Effect of plasticizers on film properties, drug permeation and drug release from coated tablets. *International Journal of Pharmaceutics*. 333(1), 34-44.
54. Mali S., Grossmann M.V.E., García M.A., Martino M.N., Zaritzky N.E., 2004. Barrier, mechanical and optical properties of plasticized yam starch films. *Carbohydrate Polymers*. 56(2), 129-135.
55. Kurt A., Kahyaoglu T., 2014. Characterization of a new biodegradable edible film made from salep glucomannan. *Carbohydrate Polymers*. 104, 50-58.
56. Wilhelm H.M., Sierakowski M.R., Souza G., Wypych F., 2003. Starch films reinforced with mineral clay. *Carbohydrate Polymers*. 52(2), 101-110.



